

## Anisotropy of the many-body enhancements on the Fermi surface of Pd

W. Joss\* and G. W. Crabtree

*Materials Science and Technology Division, Argonne National Laboratory, Argonne, Illinois 60439*

(Received 25 June 1984)

A new Korringa-Kohn-Rostoker parametrization of the cyclotron effective masses in Pd based on the data reported in the preceding paper is described. The parametrization was used to derive the many-body-enhanced Fermi velocities of electrons in the high-symmetry planes on each of the four sheets of the Fermi surface, the enhanced density of states for each sheet, and the total enhanced density of states. The total enhanced density of states agrees with the value derived from specific-heat measurements to within 2.9%. Comparison of the results of the parametrization with Fermi velocities and densities of states derived from one-electron band calculations give a detailed picture of the anisotropy of the total many-body enhancement in the Fermi velocity to the density of states over the Fermi surface. Estimates of the anisotropy of the electron-electron enhancement are obtained by subtraction from the total enhancement of the electron-phonon contribution as calculated by Pinski and Butler based on the rigid muffin-tin approximation. The electron-electron enhancement obtained in this way shows considerable variation from sheet to sheet.

### I. INTRODUCTION

The role of many-body interaction in determining the properties of Pd has received considerable attention (for electron-phonon interaction, see Butler,<sup>1</sup> Pinski *et al.*,<sup>2</sup> Pinski and Butler,<sup>3</sup> Papaconstantopoulos *et al.*,<sup>4,5</sup> and Grodzicki and Appel;<sup>6</sup> for electron-electron interaction, see Gladstone *et al.*,<sup>7</sup> de Chatel and Wohlfarth,<sup>8</sup> Béal-Monod,<sup>9</sup> Diamond,<sup>10</sup> Fay and Appel,<sup>11</sup> Hertel, Appel, and Fay,<sup>12</sup> and Gyorffy *et al.*,<sup>13</sup> for experimental measurements, see R. A. Webb *et al.*,<sup>14</sup> Stritzker,<sup>15</sup> Meyer and Stritzker,<sup>16</sup> Hsaing *et al.*,<sup>17</sup> Stewart and Brandt,<sup>18</sup> Franse,<sup>19</sup> Dumoulin *et al.*,<sup>20</sup> and Zwart and Schroeder<sup>21</sup>). It is widely believed that the large Stoner enhancement of the magnetic susceptibility of Pd leads to strong spin fluctuations which suppress superconductivity and enhance the density of states at the Fermi level. Although many experiments are sensitive to the existence of spin fluctuations, no experiment has yet provided a quantitative measure of their strength in Pd. Nevertheless, Pd is often cited as a typical example of the effect of spin fluctuations on metallic properties. In many ways Pd is well suited to this role. Unlike most compounds, Pd can be prepared as pure, relatively perfect single crystals which can be well characterized experimentally. Several thorough calculations of the one-electron band structure have been made (Andersen,<sup>22</sup> Mueller *et al.*,<sup>23,24</sup> MacDonald *et al.*,<sup>25</sup> and Jarlborg and Freeman<sup>26</sup>), and the Fermi-surface properties have been extensively investigated in many experiments (see the preceding paper,<sup>27</sup> references therein, and Ohlsen *et al.*,<sup>28</sup> Roeland *et al.*,<sup>29</sup> Dye *et al.*,<sup>30</sup> Windmiller *et al.*,<sup>31</sup> and Vuillemin<sup>32</sup>). This wealth of information on the electronic structure has not yet been used in the spin-fluctuation problem, as most formulations of electron-electron interactions ignore the detailed band structure (Doniach and Engelsberg,<sup>33</sup> Berk and Schrieffer,<sup>34</sup> Brinkman and Engelsberg,<sup>35</sup> Béal-Monod *et al.*,<sup>36</sup> Schrieffer,<sup>37</sup> Béal-Monod and Lawrence,<sup>38</sup> MacDonald,<sup>39</sup> Béal-Monod

and Daniel,<sup>40</sup> Riseborough,<sup>41</sup> and Béal-Monod<sup>42</sup>).

In this paper we present a description of the variation of the many-body enhanced Fermi velocities, cyclotron effective masses, and densities of states at the Fermi level on the four sheets of the Fermi surface of Pd, based on a Korringa-Kohn-Rostoker (KKR) parametrization of the new effective masses reported by Joss *et al.* in the preceding paper. When combined with band-structure calculations, this parametrization allows us to infer the variation of the many-body enhancement over the Fermi surface (FS). Theoretical calculations of the variation of the electron-phonon contribution to the total many-body enhancement are then used to estimate the variation of the electron-electron enhancement.

### II. KKR PARAMETRIZATION

A parametrization of the effective masses based on the KKR method of band calculation using the new, more complete mass data on the open hole surface presented in the preceding paper was carried out. For completeness and increased reliability, many additional masses taken from the literature were also included in the parametrization. A total of 27 measured masses were used in the fit: ten on the open hole surface, eleven on the  $\Gamma$ -centered electron sheet, four on the  $X$ -hole pockets, and two on the  $L$ -hole pockets. The details of the parametrization scheme have been described elsewhere (Dye *et al.*,<sup>43</sup> Ketterson *et al.*,<sup>44</sup> and Shaw *et al.*<sup>45</sup>). Since no new area data were taken in this work, the same parametrization of the Fermi surface geometry as reported earlier<sup>30</sup> was used. Average masses were derived from those reported in Table I of the preceding paper by summing the values obtained at different fields according to the formula

$$m^* = \frac{\sum_i m_i^* / \sigma_i^2}{\sum_i 1 / \sigma_i^2},$$

TABLE I. Areas and cyclotron effective masses of some extremal orbits on the Fermi surface of Pd, as measured experimentally and predicted by the KKR fit. The masses were calculated with the phase-shift derivatives of fit 1 in Table II.

FS sheet, orbit	Orbit type, band	Center ( $2\pi/a$ )	Field direction	Area (a.u.)		Mass ( $m^*/m$ )	
				Expt.	KKR fit	Expt.	KKR fit
<i>L</i> holes	$h_5$	$L(\frac{1}{2}, \frac{1}{2}, \frac{1}{2})$	[100]	0.006 137 <sup>a</sup>	0.006 161	1.10 ±0.05 <sup>b</sup>	0.859
			[110]	0.005 806 <sup>a</sup>	0.005 673	0.94 ±0.05 <sup>c</sup>	0.989
			[1 $\bar{1}$ 0]	0.008 782 <sup>a</sup>	0.008 869	1.15 ±0.10 <sup>b</sup>	1.114
			[111]	0.005 090 <sup>a</sup>	0.005 046	1.10 ±0.05 <sup>b</sup>	0.904
			[1 $\bar{1}$ 1]	0.007 804 <sup>a</sup>	0.007 908	0.84 <sup>a,d</sup>	0.87 ±0.10 <sup>c</sup>
			[11 $\bar{2}$ ]	0.008 65 <sup>a</sup>	0.008 737	1.15 ±0.10 <sup>c</sup>	1.045
<i>X</i> holes	$h_4$	$X(1,0,0)$	[100]	0.015 29 <sup>a</sup>	0.015 38	0.624±0.007 <sup>e,d</sup>	0.634
			[010]	0.023 76 <sup>a</sup>	0.023 80	0.63 <sup>f,g</sup>	1.059±0.007 <sup>e,d</sup>
			[110]	0.018 39 <sup>a</sup>	0.018 47	1.04 <sup>f,h</sup>	1.03 ±0.03 <sup>c</sup>
			[011]	0.023 87 <sup>a</sup>	0.023 93	1.05 <sup>g</sup>	0.78 <sup>f,d</sup>
			[111]	0.020 05 <sup>a</sup>	0.020 08	0.79 ±0.02 <sup>c</sup>	0.78 <sup>f,d</sup>
			22° <sup>i</sup>	0.015 8 <sup>c</sup>	0.016 11	1.03 <sup>f</sup>	1.03 <sup>f</sup>
			[100]	0.731 2 <sup>a</sup>	0.728 8	0.87 <sup>f,d</sup>	0.866
			[110]	0.826 5 <sup>a</sup>	0.828 3	0.650±0.016 <sup>c</sup>	0.668
Electrons	$e_6$	$\Gamma$	[100]	0.731 2 <sup>a</sup>	0.728 8	2.02 <sup>f,d</sup>	1.883
			[110]	0.826 5 <sup>a</sup>	0.828 3	2.00 <sup>g</sup>	2.261±0.017 <sup>e,d</sup>
			[111]	0.648 0 <sup>a</sup>	0.649 1	2.30 <sup>f</sup>	1.96 <sup>f,d</sup>
			10° <sup>i</sup>		0.725 1	2.00 <sup>f,d</sup>	1.865
			25.5° <sup>i</sup>		0.722 8	2.02 <sup>f,d</sup>	2.000
			37° <sup>i</sup>		0.698 8	2.17 <sup>f,d</sup>	2.172
			61.4° <sup>i</sup>	0.646 <sup>c</sup>	0.655 6	1.936±0.020 <sup>e,d</sup>	1.999
			77° <sup>i</sup>		0.727 2	2.19 <sup>f,d</sup>	2.270
			84° <sup>i</sup>		0.789 0	2.39 <sup>f,d</sup>	2.379
			[111]	0.687 3 <sup>a</sup>	0.688 3	2.01 <sup>f,d</sup>	2.002
			61.4° <sup>i</sup>	0.678 <sup>c</sup>	0.684 5	1.944±0.051 <sup>e,d</sup>	2.023
			Open holes, $\alpha$	$h_5$	$W(\frac{1}{2}, 0, 1)$	[100]	0.071 90 <sup>a</sup>
22° <sup>i</sup>	0.077 1 <sup>c</sup>	0.076 68				2.40 <sup>f</sup>	2.62 ±0.02 <sup>e,d</sup>
Open holes, $\beta$	$h_5$	$X(1,0,0)$	[011]		0.308 2		15.56
			[111]	0.232 6 <sup>a</sup>	0.233 4		7.17
			61.4° <sup>i</sup>	0.218 <sup>c</sup>	0.219 8	6.61 ±0.05 <sup>e,d</sup>	6.69
			76° <sup>i</sup>	0.240 <sup>c</sup>	0.242 1	8.96 ±0.21 <sup>e,d</sup>	8.88
			77.6° <sup>i</sup>	0.246 <sup>c</sup>	0.249 0	9.25 ±0.18 <sup>e,d</sup>	9.47
Open holes, $\beta'$	$h_5$	$X(0,1,0)$	61.4° <sup>i</sup>	0.252 <sup>c</sup>	0.254 3	7.94 ±0.11 <sup>e,d</sup>	8.03
Open holes, $\gamma$	$h_5$	$S[011]^j$	[011]	0.201 8 <sup>a</sup>	0.202 6	5.90 ±0.05 <sup>e,d</sup>	6.08
						6.0 <sup>f</sup>	
						5.8 <sup>a</sup>	
			61.4° <sup>i</sup>	0.282 <sup>c</sup>	0.280 6	9.97 ±0.24 <sup>e,d</sup>	9.70
			7.21 ±0.15 <sup>e,d</sup>	6.99			
			7.21 ±0.15 <sup>e,d</sup>	6.99			
			0.217 <sup>c</sup>	0.219 7	6.66 ±0.06 <sup>e,d</sup>	6.77	
Open holes, $\epsilon$	$e_5$	$\Gamma$	[100]		1.969 1		11.47

<sup>a</sup>Dye *et al.* (Ref. 30).<sup>b</sup>Brown *et al.* (Ref. 48).<sup>c</sup>Ernest *et al.* (Ref. 49).<sup>d</sup>Used in KKR fit.<sup>e</sup>Preceding paper (Ref. 27).<sup>f</sup>Windmiller *et al.* (Ref. 31).<sup>g</sup>Venema (Ref. 51).<sup>h</sup>See footnote 50.<sup>i</sup>Angle from [100] in (01 $\bar{1}$ ).<sup>j</sup>Non-central orbit.

where  $\sigma_i$  is the error quoted in Table I of the preceding paper, and the subscript  $i$  distinguishes measurements at different fields. The error of the average mass was computed by the formula

$$\sigma = \left[ \sum 1/\sigma_i^2 \right]^{-1/2}.$$

Table I shows the average masses and errors derived from the preceding paper as well as masses found in earlier experimental work. The masses were fit by minimizing the weighted least-square error

$$\Delta = \sum_i W_i \left[ \frac{m_{\text{expt},i}^* - m_{\text{KKR},i}^*}{m_{\text{expt},i}^*} \right]^2 + W_N \left[ \frac{N_{\text{expt}} - N_{\text{KKR}}}{N_{\text{expt}}} \right]^2, \quad (1)$$

where the subscript  $i$  refers to different cyclotron orbits, and  $N_{\text{expt}}$  and  $N_{\text{KKR}}$  are the total electronic density of states at the Fermi level measured by specific-heat experiments and calculated from the KKR fit to the measured masses, respectively. The weighting factors  $W_i$  for the masses were set equal to  $(m_{\text{expt},i}^*/\sigma_i)^2$ , where  $\sigma_i$  is the error of the mass measurement. For previous experimental work where error bars on the masses are not given, an arbitrary error of 3% was assigned to all masses except the  $L$ -centered pockets, which were assigned a 10% error because of the unusual experimental difficulty of measuring the amplitude of such a low-frequency oscillation.

The error function (1) and weighting factors  $W_i$  are identical to that used earlier by Dye *et al.*, except that in the earlier work the errors  $\sigma_i$  were arbitrarily set equal to 1. Setting  $\sigma_i$  to the experimental uncertainty in each mass is more appropriate for fitting the orbital data, since it allows the deviation of the KKR mass from the measured mass for each orbit to be correlated with the experimental error. However, the density of states computed from such a fit may not be so reliable because the open hole sheet, which is responsible for  $\sim 87\%$  of the density of states, is not heavily weighted in the mass fit due to the relatively large experimental errors associated with its masses. To reduce this problem, the experimental density of states measured by specific-heat experiments (Boerstael *et al.*<sup>46</sup>) was included in Eq. (1) as an additional piece of data to be fit on the same basis as one of the masses. Its weighting factor  $W_N$  was used as a variable parameter to change the relative emphasis given to the orbital masses and surface-averaged density of states in Eq. (1) without changing the relative weights of the orbital masses themselves. Because the density of states is determined mostly by the open hole sheet, changing  $W_N$  affects the KKR masses of the open hole orbits much more than those on other sheets.

### III. RESULTS

#### A. Density of states at the Fermi level

Fits made with various values of  $W_N$  showed that there is a shallow minimum in the quality of the fit to the masses as a function of  $W_N$  or, equivalently, as a function

of  $N_{\text{KKR}}$ . A fit to the masses alone ( $W_N=0$ ) produced KKR masses with an rms error of 3.2%, while a fit which was forced to give the experimental density of states ( $W_N=10^4$ ) predicted masses with an rms error of 4.3%. This suggests that the measured masses are consistent with a range of values of the density of states. To investigate this possibility quantitatively, a series of fits was made with  $W_N=10^4$  at various values of the parameter  $N_{\text{expt}}$ . (With such a large  $W_N$ , the fit always gives  $N_{\text{KKR}}=N_{\text{expt}}$ .) The rms error of the KKR masses in such a fit indicates how far the KKR masses must deviate from the experimental values in order to produce a given density of states. The results are shown in Fig. 1. As can be seen there, the error in the masses is minimized for a density of states about 5% below the experimental value. The fit giving the minimum error in the masses is identical to that obtained for  $W_N=0$ . Forcing  $N_{\text{KKR}}$  to a slightly higher value does not significantly worsen the fit to the masses. In fact, the fit to the masses on the open hole sheet is initially *improved* by forcing  $N_{\text{KKR}}$  closer to the specific-heat value, as shown by the curve labeled "open hole orbits" in Fig. 1. This can be understood by noting that the open hole masses account for about 40% of the masses in the fit, but contribute 87% of the density of states. Fitting the more numerous low-mass orbits well requires the high-mass orbits to be fit with too-small values, and the resulting KKR density of states is too low. The best fit to the open hole masses only has a density of states 2.9% below experiment. This discrepancy is of the same order as is found in other metals where KKR fits have been made (Shaw *et al.*,<sup>45</sup> Dye *et al.*,<sup>43</sup> and Crabtree *et al.*<sup>47</sup>).

From the above discussion we conclude that the masses measured by the dHvA effect at high field are consistent with the density of states measured by specific-heat experiments at zero field in Pd. Because of the inherent uncer-

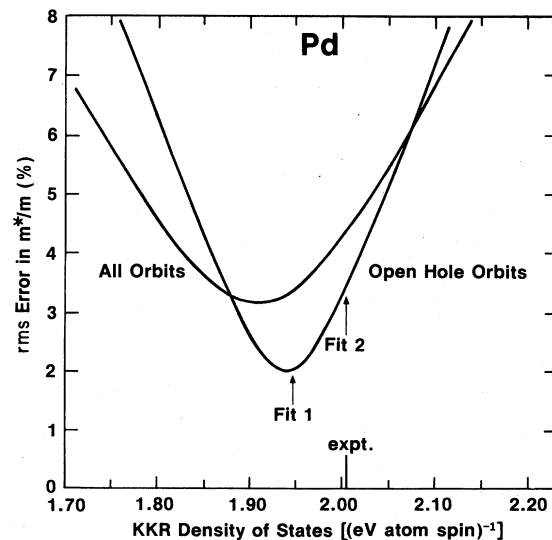


FIG. 1. rms error in the cyclotron effective masses as a function of the KKR density of states at the Fermi level. See text for explanation of how the curve was constructed.

tainties in the mass measurements, the agreement between the two quantities cannot be tested on a scale finer than a few percent. Consequently, a *small* reduction of the effective masses with field cannot be seen by this comparison.

In order to describe the orbital and surface-averaged properties of Pd, we have chosen the two fits labeled fit 1 and fit 2 in Fig. 1. In fit 1, the average error in the masses is about equal to that in the density of states and, coincidentally, fit 1 is the best fit to the open hole masses. We have chosen this fit as the best overall fit to the orbital properties. Fit 2 gives the correct experimental density of states, and has a slightly larger error in the orbital masses than does fit 1. This fit is used for comparing the surface-averaged properties measured by the dHvA effect with band-structure results to derive estimates of the electron-phonon and electron-electron enhancements.

The phase-shift derivatives  $\eta'$  derived from these two fits are quite different, as shown in Table II. Despite the relatively large differences in the phase-shift derivatives, the error in the fit to the masses in the two cases is about equal. This nonuniqueness in the  $\eta'$  has been found in mass fits to Pt (Dye *et al.*<sup>43</sup>) and the noble metals (Shaw *et al.*<sup>45</sup>) and indicates that the values of the fitting parameters  $\eta'$  do not have any physical meaning. The fact that there are different parameter sets which give fits to the masses of nearly equal quality may mean that the parameter set is underdetermined; i.e., that a good fit could be obtained with a smaller parameter set. There is no inherent reason why the same number of parameters needs to be used in the area and mass fits. For example, in Nb<sup>47</sup> only three  $\eta'$  were required to fit the masses, while five  $\eta'$  were used to fit the areas. We have not explored the possibility of fitting the masses in Pd with less than seven parameters.

### B. Cyclotron effective masses

The orbital properties of Pd as measured and parametrized by fit 1 are shown in Table I. For completeness, we also show earlier measurements of masses as reported in the literature.<sup>48–51,30,31</sup> The agreement between the various measurements is rather good, except for certain orbits on the *L*-centered hole sheet.

Although the phase shifts of Dye *et al.*<sup>30</sup> were used in calculating the Fermi-surface geometry, the parametrized areas shown in Table I differ by  $\sim 1\%$  on the *L*-centered hole orbit with the field along [111] and by 0.1% on the

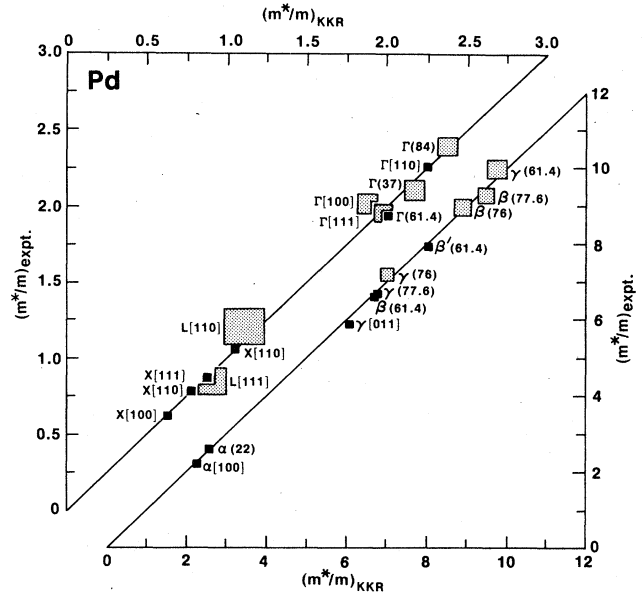


FIG. 2. Measured cyclotron effective masses  $(m^*/m)_{\text{expt}}$  vs calculated masses from the KKR fit  $(m^*/m)_{\text{KKR}}$ . The length of the edge of the square representing a given mass equals the experimental error quoted in Table I.

other orbits from those reported by Dye *et al.* This small discrepancy is due to several improvements in the orbit-tracing code which computes the orbital areas and their derivatives with respect to the phase shifts from a given set of phase shifts. Since the work of Dye *et al.*, this code was converted from single to double precision, and the iteration procedure for finding the Fermi surface was improved to give better convergence of the Fermi radius and its derivative with respect to the phase shifts. In addition, the procedure for handling free-electron singularities was improved so that reliable point properties can be computed closer to the singularity than previously. Finally, the grid size used in tracing the orbits was reduced to provide accuracy commensurate with the other improvements discussed above.

The quality of the KKR fit to the masses can be seen in Fig. 2, which shows the parametrized KKR masses versus the measured masses. The length of the edge of the square representing each mass is equal to the experimental error in the measured mass. Nearly all of the squares overlap the solid line, indicating the fit has reproduced the

TABLE II. Phase shifts and phase-shift derivatives used in the KKR parametrization of areas and cyclotron effective masses of extremal orbits on the Fermi surface of Pd.  $E_F=0.5450$  Ry;  $a=3.884$  Å. Phase shifts are in radians, phase-shift derivatives in radians per unit energy, where the unit of energy is  $(\hbar^2/2m)(2\pi/a)^2$ .

	$\Gamma_6^+$	$\Gamma_6^-$	$\Gamma_8^-$	$\Gamma_8^{+(3/2)}$	$\Gamma_7^+$	$\Gamma_8^{+(5/2)}$	$F$	$\alpha$
$\eta$	-0.3133	-0.1680	-0.0116	-0.2916	-0.3534	-0.3534	0.0011	-0.0119
Fit 1 <sup>a</sup> $\eta'$	-11.98	7.262	-1.670	1.104	0.5632	0.5632	0.5722	-8.023
Fit 2 <sup>b</sup> $\eta'$	-15.65	5.798	0.08614	1.508	0.4854	0.4854	0.6116	-12.70

<sup>a</sup>Minimizes the rms error in the masses of the open hole orbits.

<sup>b</sup>Constrained to the experimental density of states at the Fermi level,  $N_{\text{expt}}=2.004$  (states/eV atom spin) (Ref. 46).

measured masses within experimental error in most cases.

The largest deviation of the experimental and KKR masses occurs on the  $L$ -centered hole sheet. This is to be expected since these masses were assigned the largest experimental error and therefore the least weight. The angular variation of the KKR masses follows the experimental pattern very well, considering that only two of the experimental masses were used in the fit. One unusual feature of the masses on the  $L$  pockets is the violation of the rule that the angular variations in the mass follow the angular variations in the area. This reflects the nonparabolic nature of the bands caused by the van Hove singularity near the  $X$ - $L$  line. This singularity distorts the shape of the  $L$ -hole sheet from the ellipsoidal geometry expected for a small pocket, and has a strong effect on the Fermi velocities and masses as well. The unusual anisotropy in the Fermi velocities associated with the singularity is discussed in Sec. III C below. No effort was made to improve the fit to the  $L$  holes because their contribution to the density of states and number of electrons is small.

The  $X$ -centered holes were fit very well because of the small experimental error bars associated with the four masses on these sheets used in the fit. Since the bands producing these sheets contain no singularities or other anomalies, a good fit is to be expected.

The KKR masses on the  $\Gamma$ -centered sheet display an unusual anisotropy, as shown in Fig. 3. Our first fits used only five masses on this sheet and showed about 8% error at [100]. In order to improve the fit several nonsymmetry direction masses from the work of Windmiller *et al.*<sup>31</sup> were included, as shown in Table I. The inclusion of these masses did not significantly change the quality of the fit on the  $\Gamma$ -centered sheet. As shown in Fig. 3, the KKR fit follows the masses fairly well except near [100], where it is about 7% low. This feature could be due to the relatively low weight given to the [100] mass in the fit. A discussion of the anisotropy in the KKR masses in terms of the KKR Fermi velocities on the  $\Gamma$ -centered sheet is given in Sec. III C.

The KKR fit to the open hole masses is generally good, being in error by at most a few percent. The error for

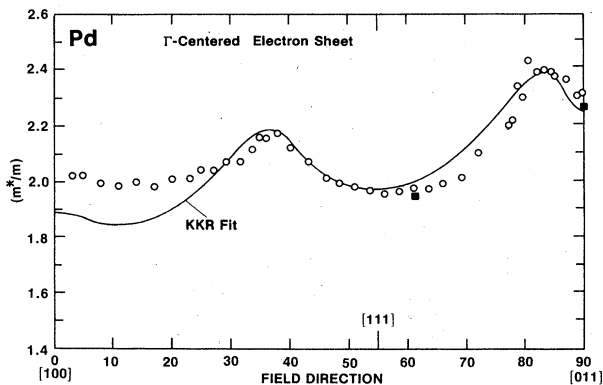


FIG. 3. Variation of the measured cyclotron effective masses (symbols) and KKR fitted masses (solid line) on the  $\Gamma$ -centered electron sheet. The open circles are taken from Windmiller *et al.* (Ref. 31), and the filled squares from the preceding paper (Ref. 27).

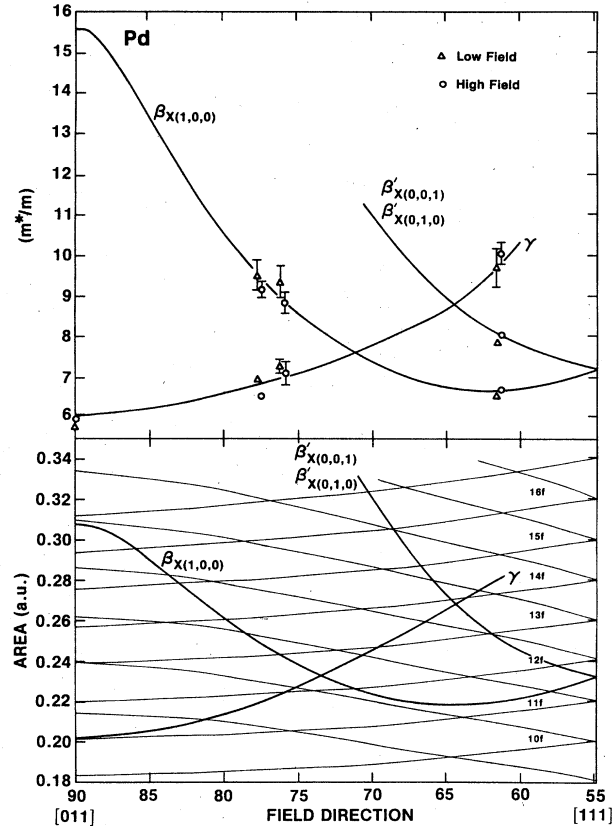


FIG. 4. Variation of the measured cyclotron effective masses (symbols) and KKR fitted masses (solid lines) for the  $\beta$  and  $\gamma$  orbits on the open hole sheet (upper part). Variation of the cross-sectional areas from the KKR fit and the interfering harmonics of the  $X$ -centered hole ellipsoids (lower part).

each measured mass is roughly equal to the experimental error. All the measured masses were used in the fit, so it is impossible to check the predictive ability of the fit by comparison with independent measurements of the mass. The angular variations of the KKR and experimental masses are shown in Fig. 4. The  $\gamma$  orbit is sampled fairly completely by the experiment, but the  $\beta$  orbit masses could be measured only away from the high-mass region near [011]. The inclusion of the experimental density of states from specific-heat measurements in the fit helps to represent these parts of the surface, since the high-mass regions contribute most strongly to the density of states.

### C. Fermi velocities

The KKR parametrization allows the measured orbital masses to be converted to Fermi velocities. These are shown in Figs. 5–8 for the high symmetry planes of each sheet. (To convert velocities in  $2\pi/a$  to SI units multiply them by  $[h/(2ma)] = 936 \text{ km/s}$  where  $a = 3.884 \text{ \AA}$ .) In general, the anisotropy of the velocity is very similar to that reported by Dye *et al.*,<sup>30</sup> but the magnitudes of the velocities are slightly different. On the  $L$ -centered holes (Fig. 5) the velocities are a few percent larger than those reported by Dye *et al.* The off-symmetry extrema in the

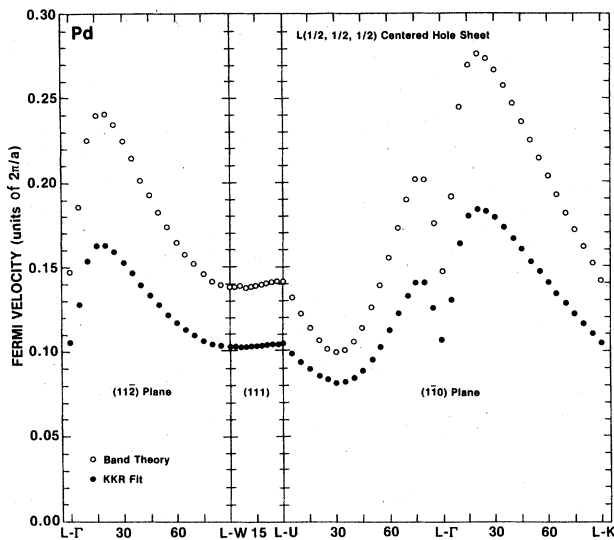


FIG. 5. Variation of the Fermi velocities on the  $L$ -centered holes of Pd as given by the KKR fit and the band-structure calculation of MacDonald *et al.* (Ref. 25).

velocities show directly that these sheets do not follow an ellipsoidal model.

The Fermi velocities for the  $X$ -centered hole sheet (Fig. 6) are a few percent higher than those reported by Dye *et al.*, but show virtually the same anisotropy.

On the  $\Gamma$ -centered electron sheet the anisotropy is different from that reported by Dye *et al.* Figure 7 shows an increase in the velocity at  $\Gamma-X$  over that at  $\Gamma-K$ , while Dye *et al.* found a fairly flat variation. The velocities in the  $\Gamma-X$  direction affect the masses of orbits near the  $[100]$  direction, because for this field direction the orbit crosses  $\Gamma-X$  the maximum number of times (four).

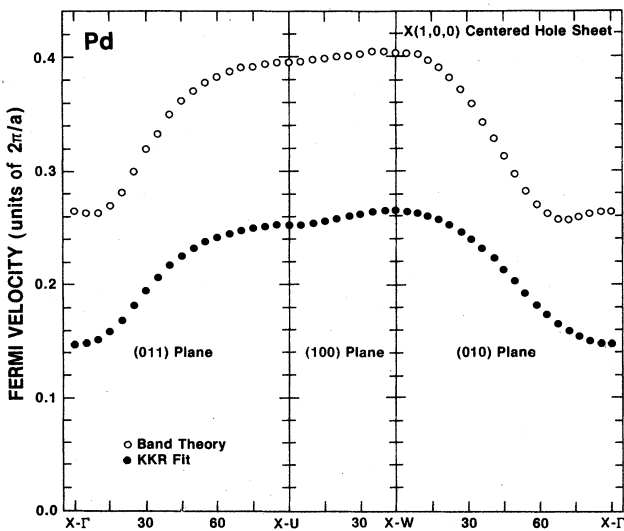


FIG. 6. Variation of the Fermi velocities on the  $X$ -centered holes of Pd as given by the KKR fit and the band-structure calculation of MacDonald *et al.* (Ref. 25).

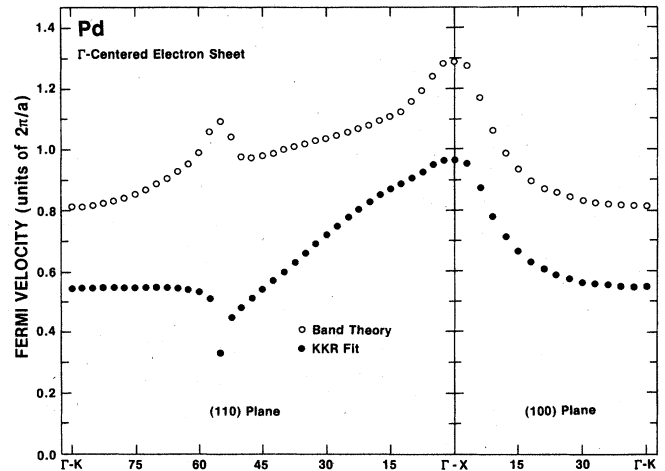


FIG. 7. Variation of the Fermi velocities on the  $\Gamma$ -centered electron sheet of Pd as given by the KKR fit and the band-structure calculation of MacDonald *et al.* (Ref. 25). The opposite variations near  $55^\circ$  may be due to a band crossing, as explained in the text.

The systematically low KKR masses near  $[100]$  suggest that the velocities near  $\Gamma-X$  are slightly too high in the present fit. Another difference from the results of Dye *et al.* is the decrease of the velocity near  $\Gamma-L$  in the  $(110)$  plane, as opposed to the increase found by Dye *et al.* As noted earlier by Dye *et al.*<sup>30</sup> and Mueller *et al.*,<sup>24</sup> the velocity at  $\Gamma-L$  and at certain other high-symmetry points is strongly affected by band crossings near the Fermi level. Near a band crossing the slope of the bands and the resulting Fermi velocity depends strongly on the degree of hybridization between the two bands, which is governed by the symmetry of the  $\vec{k}$  vector at the crossing. Crossings which occur near the Fermi level and near high-symmetry points can produce large effects in the Fermi velocities. This effect is responsible for the structure in the Fermi velocity on the  $L$ -hole sheet at  $\Gamma-L$ , on the  $X$ -hole sheet at  $\Gamma-X$ , on the  $\Gamma$ -electron sheet at  $\Gamma-X$

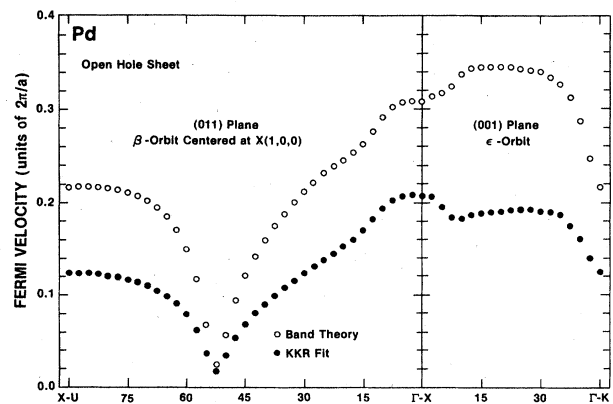


FIG. 8. Variation of the Fermi velocities on the open hole sheet of Pd as given by the KKR fit and the band-structure calculation of MacDonald *et al.* (Ref. 25).

TABLE III. Density of states on each of the four sheets of the Fermi surface of Pd as given by the KKR fits and band-structure calculations.

	$N(E_F)$ (states/eV atom spin)		Electrons	Open holes	Total
	$L$ holes (total of 4 sheets)	$X$ holes (total of 3 sheets)			
KKR fit 1 <sup>a</sup>	0.0347	0.0403	0.185	1.686	1.946
KKR fit 2 <sup>b</sup>	0.0350	0.0405	0.185	1.744	2.004
Band structure <sup>c</sup>	0.0073	0.029	0.125	1.040	1.202
Band structure <sup>d</sup>		0.028	0.124	1.130 <sup>e</sup>	1.283

<sup>a</sup>Minimizes the rms error in the masses of the open hole orbits

<sup>b</sup>Constrained to the experimental density of states at the Fermi level,  $N_{\text{expt}} = 2.004$  (states/eV atom spin) (Ref. 46).

<sup>c</sup>Andersen (Ref. 22).

<sup>d</sup>MacDonald *et al.* (Ref. 25).

<sup>e</sup>Includes contribution from  $L$  pocket, which belongs to the same band.

and  $\Gamma-L$ , and on the open hole sheet at  $\Gamma-X$ . The sensitivity of the Fermi velocity on the  $\Gamma$ -centered surface to the details of the hybridization at the band crossings can be seen by comparing Pd to Pt. In spite of their similar band structures and Fermi surfaces, the velocities in Pt dip down sharply at  $\Gamma-X$  and  $\Gamma-L$ , while in Pd the velocities jump up at these points.<sup>22,24,25,43</sup> There is no information in the orbital data used in the KKR fit that determines the nature of the hybridization at these band crossings. Therefore the Fermi velocities, having been chosen to fit the orbital masses, may not describe the actual point velocities very well near the band crossings. This failure of the KKR fitting procedure to give an accurate description of the Fermi velocities at certain points on the surface is peculiar to metals where there are band crossings near high-symmetry directions and near the Fermi level. It does not occur in the other metals where KKR fits have been made.<sup>45,47</sup>

The open hole velocities are smaller than found earlier, consistent with the higher open hole masses used in the fit and the higher density of states predicted by the fit. The anisotropy is very similar to that reported earlier.

#### D. Many-body enhancements

The densities of states for each sheet as obtained from the KKR fit and by two band-structure calculations are given in Table III. The KKR values for densities of states for each sheet are more reliable than for the Fermi velocities because they are integrals of the orbital masses, which were well described by the fit. From the ratio of the KKR values to the band-structure values, the average total enhancement due to electron-phonon and electron-electron interactions for each sheet can be derived. These are shown in Table IV for the open hole,  $\Gamma$ -centered electron, and  $X$ -hole sheets. No enhancement is given for the  $L$ -hole sheet because of the difficulty of describing it accurately in both the KKR fit and the band structure. However, comparison of the KKR and band velocities in Fig. 5 suggest a nearly constant enhancement of 1.3–1.5.

The total-enhancement parameter  $\lambda_{\text{total}} = N_{\text{KKR}}/N_{\text{BSC}} - 1$  does not vary a great deal from sheet to sheet, despite the great differences in the densities of states for each

sheet. One might expect the many-body enhancement to scale with the density of states, as is the case as one goes from metal to metal across the transition series.<sup>1,4</sup> However, a given state in a single metal couples via phonons or paramagnons to all the other states on all sheets of the Fermi surface. The enhancement for a given state is then an integral over all states on all sheets to which it couples, and depends on the densities of states of the other sheets as well as the density of states of its own sheet. In the absence of symmetry-induced selection rules or other constraints which cause the matrix elements for individual couplings to vary, there is no reason to expect much variation in the many-body effects from sheet to sheet.

The electron-phonon contribution  $\lambda_{e\text{-ph}}$  to the total enhancement has been estimated by several authors (Butler,<sup>1</sup> Papaconstantopoulos *et al.*,<sup>4,5</sup> Pinski *et al.*,<sup>2</sup> Grodzicki and Appel<sup>6</sup>). The most recent calculations give  $\lambda_{e\text{-ph}} \sim 0.41\text{--}0.47$ . Pinski and Butler<sup>3</sup> have further calculated  $\lambda_{e\text{-ph}}$  for each sheet of the Fermi surface. Their results, shown in Table IV, find even less anisotropy in  $\lambda_{e\text{-ph}}$  than in  $\lambda_{\text{total}}$ . The difference between  $\lambda_{\text{total}}$  and  $\lambda_{e\text{-ph}}$  gives an estimate of the electron-electron contribution to the mass enhancement. These values, shown in Table IV, suggest there is a large anisotropy in the electron-electron

TABLE IV. Variation of the total many-body enhancement, the electron-phonon contribution, and the difference between them on three of the four sheets of the Fermi surface of Pd. The last column gives an estimate of the electron-electron contribution.

	$\lambda_{\text{total}}^a$	$\lambda_{e\text{-ph}}^b$	$\lambda_{\text{total-eph}}$
$X$ holes	0.45	0.38	0.07
Electrons	0.49	0.41	0.08
Open holes <sup>c</sup>	0.57	0.42	0.15
Total	0.56	0.41	0.15

<sup>a</sup>Obtained from the ratio of the KKR values of fit 2 (Table III) to the band-structure values of MacDonald *et al.* (Ref. 25).

<sup>b</sup>Pinski and Butler (Ref. 3).

<sup>c</sup>Includes contribution from  $L$  holes, which belongs to the same band.

contribution, with nearly all of it coming from the open hole sheets.

#### IV. DISCUSSION AND CONCLUSIONS

We have presented a KKR parametrization of the cyclotron effective masses in Pd, using as input 27 experimental masses. The masses of orbits on the open hole sheet which contributes most of the density of states, and the masses of selected orbits on the  $X$ -centered hole and  $\Gamma$ -centered electron sheets were taken from the preceding paper. The masses of other orbits were taken from the literature. The enhanced density of states at the Fermi level predicted by this fit agrees to within a few percent with that derived from electronic specific-heat experiments (Boerstael *et al.*<sup>46</sup>).

The Fermi velocities predicted by the fit show the same qualitative variation over the Fermi surface as found earlier by Dye *et al.* Near the high-symmetry directions  $\Gamma-L$  and  $\Gamma-X$  there are band crossings near the Fermi level that produce local features in the Fermi velocities which cannot be well described by a fit based on orbital data. Because of these features we do not attempt to derive  $\vec{k}$ -dependent many-body enhancements by comparison of the KKR Fermi velocities with those computed from band-structure calculations. However, since the orbital and surface averages of the KKR velocities are not so strongly affected by local anomalies and agree well with the measured masses and electronic specific heat, we expect that averages of the Fermi velocity over individual sheets of the Fermi surface are reliable.

The separation of the total many-body enhancement into electron-phonon and electron-electron contributions is difficult, because no experiment is capable of directly measuring either contribution. Realistic calculations of the electron-electron part have not been carried out, and those for the electron-phonon part may give unreliable magnitudes because the strength of the coupling is not well known. Nevertheless, in order to obtain some information about the variation of the electron-electron contribution to the mass enhancement we have subtracted from the total the electron-phonon contribution as calculated by Pinski and Butler.<sup>3</sup> The electron-electron enhancements derived in this way must be considered as estimates whose values should be revised if the accepted values for the electron-phonon contribution change.

Assuming an enhancement due to electron-phonon interactions<sup>2</sup> of 0.41, the enhancement due to electron-electron interactions is 0.15. This is quite small compared to the enhancement in the susceptibility, which implies a Stoner factor  $S \sim 9$ . Using the expression for parabolic bands given by Riseborough,<sup>52</sup>

$$\lambda_{e-e} = \frac{9}{2} \ln(1 + S/3),$$

we expect  $\lambda_{e-e} \sim 6$ , far larger than is observed. The origin of this well-known discrepancy (de Chatel and Wohlfarth<sup>8</sup>) may be the parabolic band approximation. MacDonald<sup>39</sup> has shown that the mass enhancement in a system with finite bandwidths is smaller than that for free-electron bands, because the electron states above the top of the band cannot be coupled to electrons at the Fermi level by paramagnons. He finds that the enhancement for nearly filled bands is drastically reduced, in qualitative agreement with observations in Pd.

Despite considerable attention devoted to spin fluctuations in the past years, a quantitative understanding of their effects on the electronic specific heat,  $s$ - and  $p$ -wave pairing in superconductivity and of their dependence on magnetic field has yet to be achieved. An important theoretical advance is the demonstration that the detailed band structure can have a large effect on the spin fluctuations (MacDonald<sup>39</sup>), perhaps even changing a reduction in the susceptibility with field to an increase with field (Béal-Monod<sup>42</sup>). The estimate of the anisotropy of the electron-electron enhancement presented here further emphasizes the importance of the band structure, suggesting that the spin fluctuations are much stronger on the open hole sheet than elsewhere on the Fermi surface of Pd. These developments imply that a basic understanding of spin fluctuations in metals requires a combined approach using both band-structure and many-body calculations.

#### ACKNOWLEDGMENTS

Dr. Dale Koelling and Dr. John Ketterson have provided many useful comments and suggestions during the course of this work. This work was supported by the U. S. Department of Energy. One of us (W.J.) would like to acknowledge the sponsorship of the Schweizerischer Nationalfonds zur Förderung der wissenschaftlichen Forschung.

\*Present address: Laboratorium für Festkörperphysik, Eidgenössische Technische Hochschule, Zürich—Hönggerberg CH-8093 Zürich, Switzerland.

<sup>1</sup>W. H. Butler, Phys. Rev. **15**, 5267 (1977).

<sup>2</sup>F. J. Pinski, P. B. Allen, and W. H. Butler, Phys. Rev. Lett. **41**, 431 (1978).

<sup>3</sup>F. J. Pinski and W. H. Butler, Phys. Rev. B **19**, 6010 (1979).

<sup>4</sup>D. A. Papaconstantopoulos, L. L. Boyer, B. M. Klein, A. R. Williams, V. L. Moruzzi, and J. F. Janak, Phys. Rev. B **15**, 4221 (1977).

<sup>5</sup>D. A. Papaconstantopoulos, B. M. Klein, E. N. Economou, and L. L. Boyer, Phys. Rev. B **17**, 141 (1978).

<sup>6</sup>M. Grodzicki and J. Appel, Phys. Rev. B **20**, 3659 (1979).

<sup>7</sup>G. Gladstone, M. A. Jensen, and J. R. Schrieffer, in *Superconductivity*, edited by R. D. Parks (Marcel-Dekker, New York, 1969), Vol. 2, p. 665.

<sup>8</sup>P. F. de Chatel and E. P. Wohlfarth, Comments Solid State Phys. **5**, 133 (1973).

<sup>9</sup>M. T. Béal-Monod, Solid State Commun. **32**, 357 (1979).

<sup>10</sup>Joshua B. Diamond, Int. J. Magn. **2**, 241 (1972).

<sup>11</sup>D. Fay and J. Appel, Phys. Rev. B **16**, 2325 (1977).

<sup>12</sup>P. Hertel, J. Appel, and D. Fay, Phys. Rev. B **22**, 534 (1980).

<sup>13</sup>B. L. Gyorffy, A. Pindor, and W. M. Temmerman, Phys. Rev. Lett. **43**, 1343 (1979).



- <sup>14</sup>R. A. Webb, J. B. Ketterson, W. P. Halperin, J. J. Vuillemin, and N. B. Sandesara, *J. Low Temp. Phys.* **32**, 659 (1978).
- <sup>15</sup>B. Stritzker, *Phys. Rev. Lett.* **42**, 1769 (1979).
- <sup>16</sup>J. D. Meyer and B. Stritzker, *Phys. Rev. Lett.* **48**, 502 (1982).
- <sup>17</sup>T. Y. Hsiang, J. W. Reister, H. Weinstock, G. W. Crabtree, and J. J. Vuillemin, *Phys. Rev. Lett.* **47**, 523 (1981).
- <sup>18</sup>G. R. Stewart and B. L. Brandt, *Phys. Rev. B* **28**, 2266 (1983).
- <sup>19</sup>J. J. M. Franse, *J. Magn. Mater.* **31–34**, 819 (1983).
- <sup>20</sup>L. Dumoulin, P. Nedellec, and P. M. Chaikin, *Phys. Rev. Lett.* **47**, 208 (1981).
- <sup>21</sup>J. W. Zwart and P. A. Schroeder, *J. Phys. F* (to be published).
- <sup>22</sup>O. K. Andersen, *Phys. Rev. B* **2**, 883 (1970).
- <sup>23</sup>F. M. Mueller, A. J. Freeman, J. O. Dimmock, and A. M. Furdyna, *Phys. Rev. B* **1**, 4617 (1970).
- <sup>24</sup>F. M. Mueller, A. J. Freeman, and D. D. Koelling, *J. Appl. Phys.* **41**, 1229 (1970).
- <sup>25</sup>A. H. MacDonald, J. M. Daams, S. H. Vosko, and D. D. Koelling, *Phys. Rev. B* **23**, 6377 (1981).
- <sup>26</sup>T. Jarlborg and A. J. Freeman, *Phys. Rev. B* **23**, 3577 (1981).
- <sup>27</sup>W. Joss, L. N. Hall, G. W. Crabtree, and J. J. Vuillemin, preceding paper, *Phys. Rev. B* **30**, 5637 (1984).
- <sup>28</sup>H. Ohlsen, P. Gustafsson, L. Nordborg, and S. P. Hörnfeldt, *Phys. Rev. B* **29**, 3022 (1984).
- <sup>29</sup>L. W. Roeland, J. C. Wolfrat, D. K. Mak, and M. Springford, *J. Phys. F* **12**, L267 (1982).
- <sup>30</sup>D. H. Dye, S. A. Campbell, G. W. Crabtree, J. B. Ketterson, N. B. Sandesara, and J. J. Vuillemin, *Phys. Rev. B* **23**, 462 (1981).
- <sup>31</sup>L. R. Windmiller, J. B. Ketterson, and S. Hörnfeldt, *Phys. Rev. B* **3**, 4213 (1971).
- <sup>32</sup>J. J. Vuillemin, *Phys. Rev.* **144**, 396 (1966).
- <sup>33</sup>S. Doniach and S. Engelsberg, *Phys. Rev. Lett.* **17**, 750 (1966).
- <sup>34</sup>N. F. Berk and J. R. Schrieffer, *Phys. Rev. Lett.* **17**, 433 (1966).
- <sup>35</sup>W. F. Brinkman and S. Engelsberg, *Phys. Rev.* **169**, 417 (1968).
- <sup>36</sup>M. T. Béal-Monod, Shang-Keng Ma, and D. R. Fredkin, *Phys. Rev. Lett.* **20**, 929 (1968).
- <sup>37</sup>J. R. Schrieffer, *J. Appl. Phys.* **39**, 642 (1968).
- <sup>38</sup>M. T. Béal-Monod and J. M. Lawrence, *Phys. Rev. B* **21**, 5400 (1980).
- <sup>39</sup>A. H. MacDonald, *Phys. Rev. B* **24**, 1130 (1981).
- <sup>40</sup>M. R. T. Béal-Monod and E. Daniel, *Phys. Rev. B* **27**, 4467 (1983).
- <sup>41</sup>Peter S. Riseborough, *Phys. Rev. B* **27**, 5775 (1983).
- <sup>42</sup>M. T. Béal-Monod, *Physica*, **109&110 B**, 1837 (1982).
- <sup>43</sup>D. H. Dye, J. B. Ketterson, and G. W. Crabtree, *J. Low Temp. Phys.* **30**, 813 (1978).
- <sup>44</sup>J. B. Ketterson, D. D. Koelling, J. C. Shaw, and L. R. Windmiller, *Phys. Rev. B* **11**, 1447 (1975).
- <sup>45</sup>J. C. Shaw, J. B. Ketterson, and L. R. Windmiller, *Phys. Rev. B* **5**, 3894 (1972).
- <sup>46</sup>B. M. Boerstol, J. J. Zwart, and J. Hansen, *Physica* **54**, 442 (1971).
- <sup>47</sup>G. W. Crabtree, D. H. Dye, D. P. Karim, D. D. Koelling, and J. B. Ketterson, *Phys. Rev. Lett.* **42**, 390 (1979).
- <sup>48</sup>C. R. Brown, J. P. Kalejs, F. D. Manchester, and J. M. Perz, *Phys. Rev. B* **6**, 4458 (1972).
- <sup>49</sup>D. Ernest, W. Joss, and E. Walker, *Physics of Transition Metals, 1980*, edited by P. Rhodes (IOP, London, 1981), p. 463; D. Ernest and W. Joss (unpublished).
- <sup>50</sup>Table III of Windmiller *et al.* (Ref. 31) contains a misprint for the *X*-centered hole pocket for the field along [100] where the mass recorded as 1.360 should be 1.036.
- <sup>51</sup>W. J. Venema, Ph.D. thesis, Vrije Universiteit, Amsterdam, 1980.
- <sup>52</sup>P. S. Riseborough, *Phys. Status Solidi (B)*, **122**, 161 (1984).